

## Preparation and Ionic Conductivities of Tunnel-Type Oxides $\text{Na}_{0.80}\text{M}_{0.40}\text{Ti}_{1.60}\text{O}_4$ ( $\text{M}=\text{Co}^{\text{II}}, \text{Ni}^{\text{II}}$ )

Yu-Ju Shin,<sup>\*</sup> Mi-Hyae Park, and Seokwon Yoon<sup>†</sup>

*Dept. of Chemistry, the Catholic Univ. of Korea, Buchon 420-743, Kyeonggi, Korea*

*<sup>†</sup>Dept. of Physics, the Catholic Univ. of Korea, Buchon 420-743, Kyeonggi, Korea*

*Received May 30, 2000*

A number of quaternary oxides have been known to crystallize in one-dimensional structures such as hollandite, priderite and  $\text{CaFe}_2\text{O}_4$ .<sup>1</sup> In these structures double blocks of octahedra are formed by edge-share and developed in lattice to form one-dimensional tunnels, where alkali or alkaline earth metals are placed. With existence of vacancies, alkali metal ions in such tunnel structures are susceptible of being highly mobile, leading to ionic conductivities.

$\text{Na}_x\text{Fe}_x\text{Ti}_{2-x}\text{O}_4$  ( $0.72 \leq x \leq 0.90$ ), reported by Mumme and Reid,<sup>2</sup> has a similar structure, with Z-shaped double blocks and double tunnels (Figure 1).  $\text{Na}^+$  ions are placed in distorted trigonal prisms which are face-shared one another along **b**-axis, so that they may move within the tunnels. Systematic syntheses of isostructural oxo-fluorides  $\text{Na}_{0.5}\text{M}_{0.5}\text{Ti}_{1.5}\text{O}_{3.5}\text{F}_{0.5}$  ( $\text{M}=\text{Mg}, \text{Ni}, \text{Co}, \text{Zn}, \text{Cu}$ ) were reported earlier,<sup>3</sup> and their ionic conduction properties were also investigated.<sup>4</sup> On the other hand, the electrical conduction studies on the original phase,  $\text{Na}_x\text{Fe}_x\text{Ti}_{2-x}\text{O}_4$  ( $x=0.875$ ) and its Na-extracted or Ti-substituted phases have been studied rather recently.<sup>5-7</sup> It was evidenced that  $\text{Na}^+$ -ion is mobile within tunnels and a mixed conduction was found for Na-extracted phases due to the partial oxidation of  $\text{Fe}^{3+}$  to  $\text{Fe}^{4+}$ . However, it appears necessary to prepare new materials susceptible to have pure ionic conduction, instead of mixed one, for understanding the ionic transport features in this structure more in detail. In the present paper, we report the preparation of one-dimensional compounds  $\text{Na}_{0.80}\text{M}_{0.40}\text{Ti}_{1.60}\text{O}_4$  ( $\text{M}=\text{Co}^{\text{II}}, \text{Ni}^{\text{II}}$ ) and their ionic conductivity properties.

$\text{M}=\text{Co}^{\text{II}}, \text{Ni}^{\text{II}}$ ) and their ionic conductivity properties.

### Experimental Section

Polycrystalline samples of composition  $\text{Na}_{0.80}\text{M}_{0.40}\text{Ti}_{1.60}\text{O}_4$  ( $\text{M}=\text{Co}^{\text{II}}, \text{Ni}^{\text{II}}$ ) were prepared by direct solid state reactions using the appropriate amounts of  $\text{Na}_2\text{CO}_3$ , NiO (or CoO) and  $\text{TiO}_2$ . An excess amount of sodium carbonate (10-12 mol%) was added to compensate for the loss due to the volatilization of sodium component. The mixture was ground using a mortar and calcined at 973 K for 12 hrs, then the powder was uniaxially pressed at 80 MPa into a pellet 13 mm in diameter. The pellet was heated at 1423 K for 36 hrs with two or three times of intermittent grindings. All the thermal treatments were made under Ar atmosphere to avoid an eventual oxidation of  $\text{M}^{2+}$  to  $\text{M}^{3+}$ . The obtained products were leached into MeOH to remove the unreacted sodium components and dried under vacuum.

Identification of crystalline phases and determination of lattice parameters were carried out by X-ray powder diffraction (XRD) analysis using a Siemens D5005 diffractometer equipped with curved graphite monochromator with  $\text{CuK}\alpha$  radiation and by a computer program based on a least-square-method. For electrical conductivity measurements, the pellets ( $d=7$  mm,  $t=2$  mm) were sintered at 1443 K for 12 hrs. Blocking electrodes were deposited on both sides of the pellets by silver paste. The conductivity was obtained every 30 K at the range of 530-873 K under argon flow by AC measurements with HP 4192A LF impedance analyzer at the frequency range of 5 Hz-13 MHz. Resistance values were derived by interpretation of the complex impedance diagrams.

### Results and Discussion

**XRD results.** XRD patterns of both samples are shown in Figure 2. All the peaks were successfully indexed with the orthorhombic lattice parameters, confirming they are isostructural with  $\text{Na}_x\text{Fe}_x\text{Ti}_{2-x}\text{O}_4$ . Co-phase was found to have a unit cell slightly larger than Ni-phase, mainly due to the large ionic radius of  $\text{Co}^{2+}$  (0.745; HS) with respect to  $\text{Ni}^{2+}$  (0.69).<sup>8</sup> It is worth noting that Co-phase has also a larger cross section area  $a^*c$  to  $[010]$  direction.

**$\text{Na}_{0.80}\text{Co}_{0.40}\text{Ti}_{1.60}\text{O}_4$ .** In order to estimate the electronic contribution to the conductivity observed here, the measurements such as DC-polarization (at 1.0 V) and 4-probe DC conductivity were additionally performed, confirming that

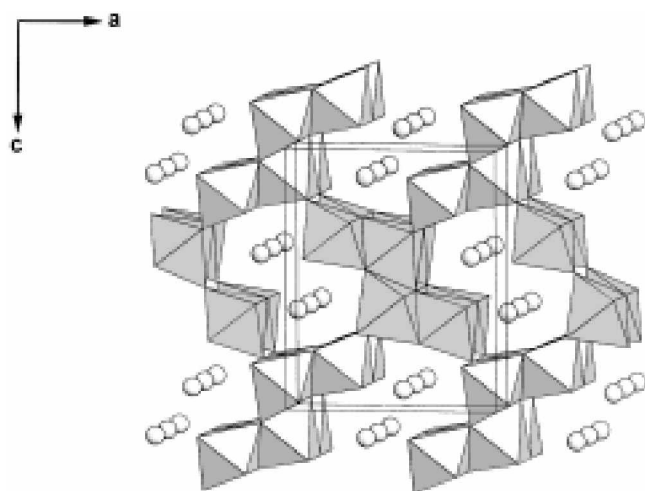


**Figure 1.** Structure of  $\text{Na}_x\text{Fe}_x\text{Ti}_{2-x}\text{O}_4$  ( $0.72 \leq x \leq 0.90$ ).  $\text{Fe}^{3+}$  and  $\text{Ti}^{4+}$  ions are considered as statistically distributed in octahedral sites and  $\text{Na}^+$  ions (balls) are partially present in the tunnel along **b**-axis.

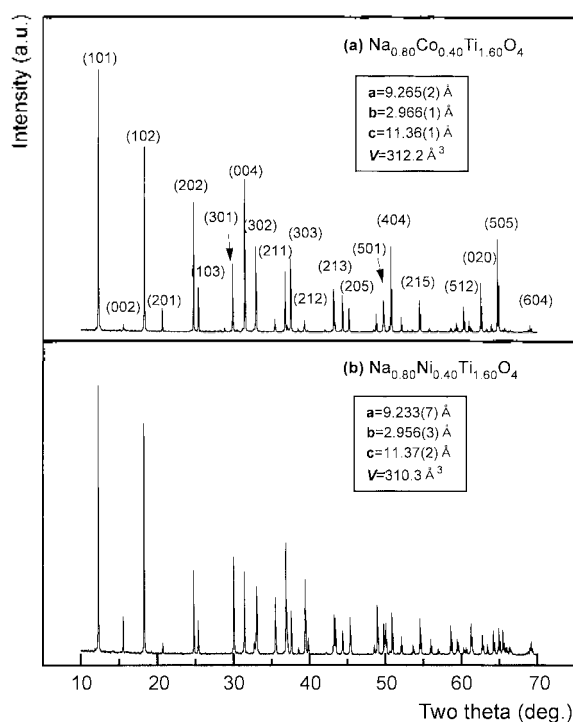


Figure 2. Powder X-ray diffraction patterns of  $\text{Na}_{0.80}\text{M}_{0.40}\text{Ti}_{1.60}\text{O}_4$  ( $\text{M}=\text{Co}$  or  $\text{Ni}$ ). Some selected peaks are labeled with Miller index.

the conduction in both samples is essentially of ionic one.

The Cole-Cole diagrams of  $\text{Na}_{0.80}\text{Co}_{0.40}\text{Ti}_{1.60}\text{O}_4$  sintered pellet, giving the imaginary part  $Z''$  of the complex imped-

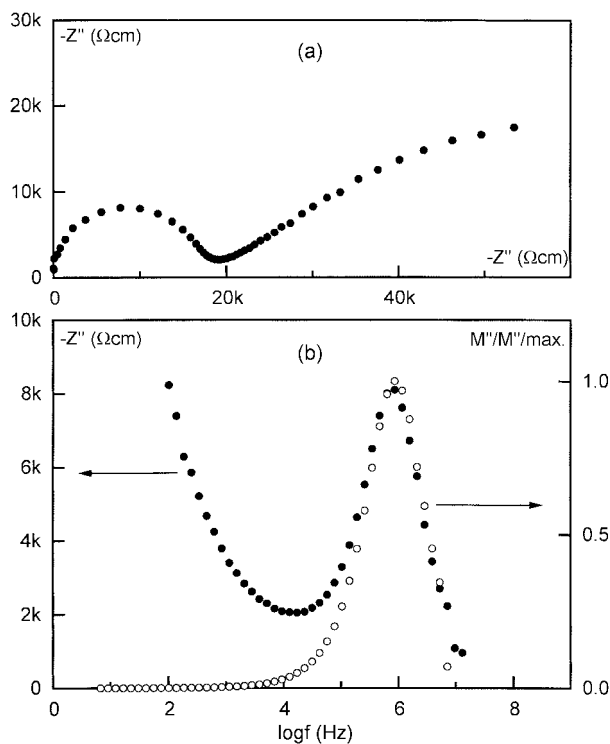


Figure 3. Cole-Cole diagram of  $\text{Na}_{0.80}\text{Co}_{0.40}\text{Ti}_{1.60}\text{O}_4$  at 682 K (a) and combined  $Z''$  and normalized  $M''$  plots as a function of frequency (b).

ance  $Z'$  as a function of its real part were obtained at various temperatures. At 682 K, for example, it shows clearly one semicircle (Figure 3(a)), of which radius increases with temperature. Figure 3(b) shows a combined  $Z''$  and normalized  $M''$  ( $M''/M''_{\text{max}}$ ) plot as a function of frequency.  $M''$  has a similar frequency-dependence with the imaginary part of dielectric permeability  $\epsilon''$ , and is known to emphasize the component with small capacitance, which corresponds to the bulk component.<sup>9</sup>  $M''$  plot exhibits a single Debye-like peak with the same frequency maximum with  $Z''$  around 870 kHz. This means that the semicircle can be ascribed to pure bulk component and the arc observed at low frequency would result from the grain boundary and electrode polarization contributions. The bulk ohmic resistance was determined from the intercept  $Z_0$  on the real axis of the zero phase angle extrapolation from the high-frequency side and the conductivity  $\sigma$  is obtained from  $Z_0$  by means of the relation  $\sigma = (1/Z_0)(e/S)$ , where  $(e/S)$  is the sample geometric factor. Frequency dependence of the normalized imaginary part of  $M''/M''_{\text{max}}$  for  $\text{Na}_{0.80}\text{Co}_{0.40}\text{Ti}_{1.60}\text{O}_4$ , at various temperatures is given in Figure 4(a). The modulus peak shifts towards higher frequencies as temperature increases, but the shape and full width at half height (FWHM) of  $M''/M''_{\text{max}}$  ( $1.25 \pm 0.02$  decades) are not changed.

The  $M''/M''_{\text{max}}$  curves are slightly non-symmetric, suggest-

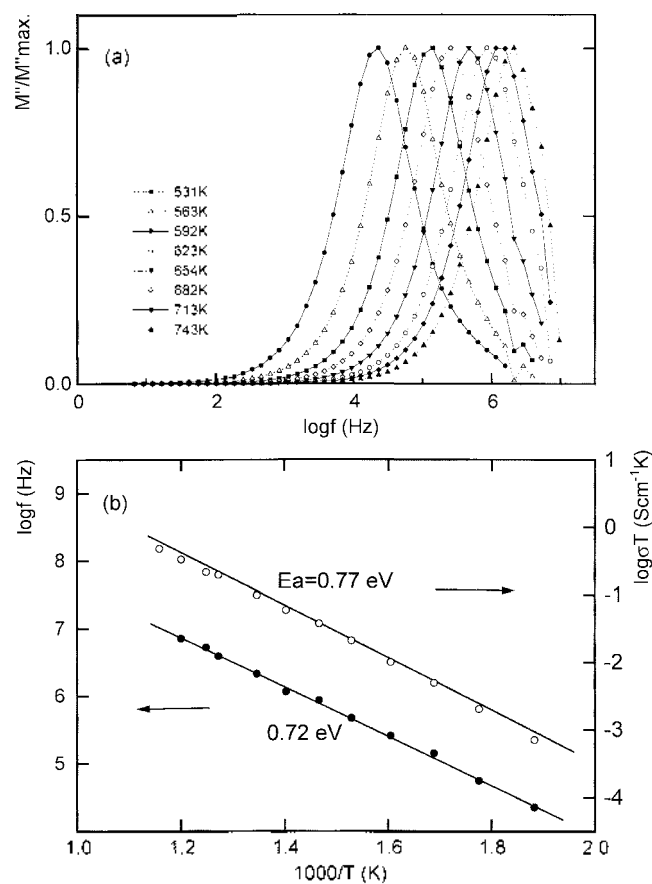
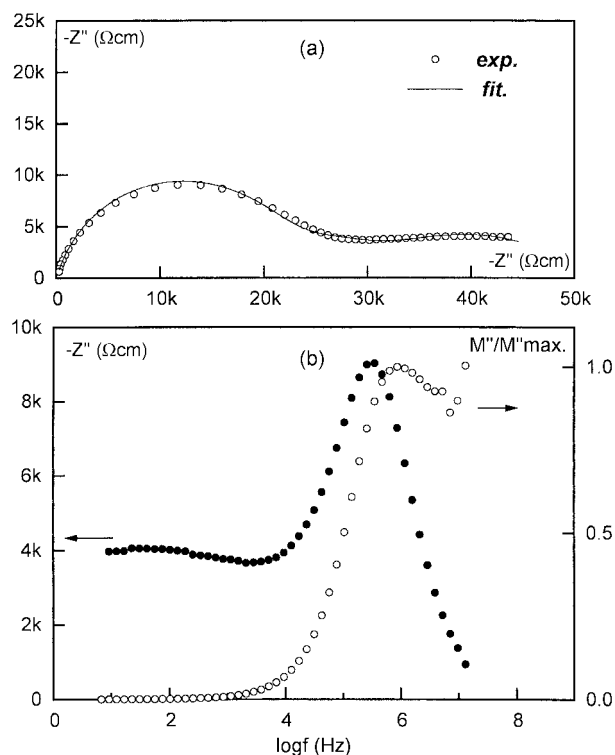


Figure 4. Normalized  $M''$  vs.  $\log f$  (Hz) of  $\text{Na}_{0.80}\text{Co}_{0.40}\text{Ti}_{1.60}\text{O}_4$  at various temperatures (a) and plots of  $\log T$  and  $\log f_{\text{max}}$  (Hz) vs.  $1000/T$  (K) (b).

ing a non-exponential behavior of conductivity relaxation that can be described by the Kohlrausch function,  $\varphi(t) = \exp[-(t/\tau_\sigma)^\beta]$ , where  $\tau_\sigma$  is the relaxation time and  $\beta$  the Kohlrausch parameter.<sup>10,11</sup>  $\beta$  was determined as  $0.90 \pm 0.02$  at each temperature, by dividing the FWHH by the Debye breadth, 1.14 decades. The  $\beta$  parameter can be interpreted as representative of a distribution of relaxation times generating the dispersive properties of materials studied.<sup>10</sup> So the small deviation of  $\beta$  from 1.0 would imply that the relaxation time distribution in  $\text{Na}_{0.80}\text{Co}_{0.40}\text{Ti}_{1.60}\text{O}_4$  is slightly wider than the Debye-type relaxation. The inverse temperature dependencies of  $\log(\sigma T)$  and  $\log f_{\max}$  ( $f_{\max} = 1/2\pi\tau_\sigma$ ) are shown in Figure 4(b). Each linear fit of  $\sigma T = \sigma_0 \exp(-\Delta E_\sigma/kT)$  and of  $f_{\max} = f_0 \exp(-\Delta E_f/kT)$  shows an Arrhenius-type behavior with correlation coefficients  $r_\sigma = 0.999$  and  $r_f = 0.989$ , respectively. The two plots exhibit the close activation energies  $\Delta E_\sigma$  and  $\Delta E_f$ , suggesting that the  $\text{Na}^+$  ion transport is mainly due to a thermally activated hopping mechanism.<sup>11,12</sup>

**$\text{Na}_{0.80}\text{Ni}_{0.40}\text{Ti}_{1.60}\text{O}_4$ .** The Cole-Cole diagram of complex impedance and  $Z''$ ,  $M''/M''_{\max}$  plot against  $\log f$  (Hz) at 800 K are present in Figure 5(a). In contrast to Co-phase. The peak frequency  $f_{\max}$  is apparently mismatched for  $Z''$  and  $M''/M''_{\max}$ . Consequently the semicircle of the Cole-Cole diagram should not be regarded as a pure bulk component, but grain boundary component being also included therein. The experimental semicircle is displaced below the real axis as generally observed in most ceramic materials,<sup>9</sup> indicating the presence of distributed elements in this material. Therefore, in order to estimate the bulk and grain boundary con-



**Figure 5.** Cole-Cole diagram of  $\text{Na}_{0.80}\text{Ni}_{0.40}\text{Ti}_{1.60}\text{O}_4$  at 800 K with the fitting-curve (a) and combined  $Z''$  and normalized  $M''/M''_{\max}$  plots as a function of frequency (b).

ductivities separately a model-circuit of three ZC elements in a serial array  $(RC)_b(RC)_{g.b.}(RC)_{dl}$  including CPE (constant phase element) was adopted, each corresponding to the ionic conductive paths in bulk, grain boundary and double layer of electrode/electrolyte.<sup>9,13</sup> Here, ( ) designates the elements therein run parallel. In each component the impedance  $Z_j^*$  is expressed as  $Z_j^* = R_j - i(\omega c_j)^{\Phi_j}$ , where  $R_j$ ,  $c_j$ , and  $\Phi_j$  represent resistance, capacitance and distribution factor of  $j$ -th component respectively. All the parameters have been determined for each temperature by fitting the experimental data using a fitting program LEVM 7.1., based on complex non-linear least square method.<sup>14</sup> Within the temperature range investigated, the bulk and grain boundary capacitances were determined as of 100-300 pF and 200-400 nF, and  $\Phi_{\text{bulk}}$  values ranges 0.83-0.86. Although the bulk capacitance is larger than the conventional value of ceramic materials ( $\sim 10^1$  pF), its magnitude  $10^{-3}$  times smaller than the grain-boundary capacitance supports this estimation.<sup>9</sup> The FWHH of  $M''/M''_{\max}$  could not be determined because the plots were not well-defined at high-frequency region, but the estimation from the half width of low-frequency region implies that the FWHH would be much larger than 1.14 decades, leading to a smaller  $\beta$  than with Co-phase, as reflected in  $\Phi$  values.

$\log(\sigma T)$  of bulk and grain boundary components and  $\log f_{\max}$  are plotted as a function of inverse temperature in Figure 6. All three plots exhibit good Arrhenius relations with  $r = 0.98$ -0.99. Considering  $f_{\max}(M'')$  is primarily related with the relaxation time  $\tau_\sigma$  of the bulk component, the close values of  $\Delta E_{\sigma(\text{bulk})}$  and  $\Delta E_f$  strongly suggests that the bulk conduction also occurs mainly through a thermally activated hopping mechanism like in Co-phase.

**$\text{Na}_{0.80}\text{Co}_{0.40}\text{Ti}_{1.60}\text{O}_4$  vs.  $\text{Na}_{0.80}\text{Ni}_{0.40}\text{Ti}_{1.60}\text{O}_4$ .** Both compounds seems to transport  $\text{Na}^+$  ions mainly by hopping mechanism, but Co-phase was found to have higher conductivities with smaller activation energies than Ni-phase. Because both compounds have the same framework and vacancy concentration, their ionic transport features would be compared mainly through two viewpoints, bond nature of Na-O and

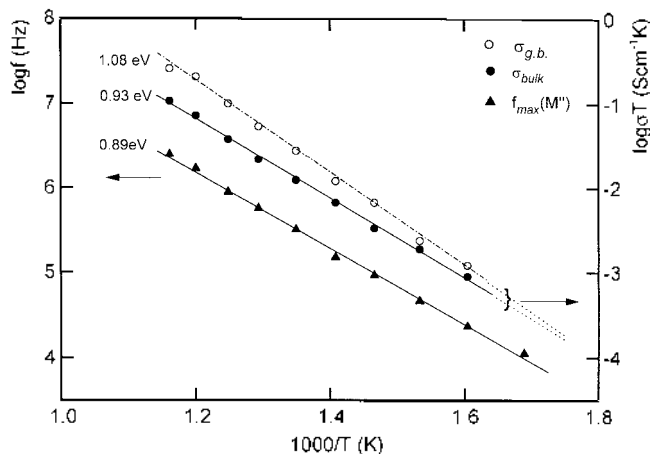


**Figure 6.** Normalized  $M''$  vs.  $\log f$  (Hz) of  $\text{Na}_{0.80}\text{Ni}_{0.40}\text{Ti}_{1.60}\text{O}_4$  at various temperatures (a) and plots of  $\log T$  and  $\log f_{\max}$  (Hz) vs.  $1000/T$  (K).

diffusion pathway of Na<sup>-</sup> in material.

Firstly, the bond character of Na-O may be compared by competitive interaction of Na-O-M: the ionic-covalency of counter-bond M-O should influence directly to the nature of Na-O. The covalency of a bond M-O may be compared following Pauling's formula  $f_c(M-O) = \{-0.25 \cdot \exp(\chi_M - \chi_O)^2\}$ , where  $\chi$  is the electronegativity.<sup>15,16</sup> Since  $\chi$  value of Ni<sup>2+</sup> is known as slightly larger (1.57) than Co<sup>2+</sup> (HS; 1.54),<sup>17</sup> Na-O in Ni-phase would be regarded as more ionic and therefore more favorable to the ionic conduction than Co-phase. However, the latter exhibits a larger unit-cell volume and cross section  $a \cdot c$  with respect to the former, being able to furnish more spacious diffusion pathway of Na<sup>-</sup> ions along  $b$  axis. Considering the relatively small difference of cell dimension between two compounds, the higher ionic transport properties of Co-phase seems to suggest that the cell dimension might be more a important factor than the ionicity of Na-O for the ion conduction.

**Acknowledgment.** This work was supported by the research fund (2000-0137) of the Catholic University of Korea.

### References

1. Post, J. E.; von Dreele, R. B.; Buseck, P. R. *Acta Crystallogr.* **1982**, B28, 1056.
2. Reid, A. F.; Mumme, W. G. *Acta Crystallogr.* **1968**, B24, 625.
3. Mayer, M.; Perez, G. C. R. *Acad. Sci. Paris.* **1974**, 278, 343.
4. Reau, J. M.; Moali, J.; Mayer, M.; Perez, G. *Rev. Chim. Miner.* **1976**, 13, 446.
5. Archambault, F.; Choynet, J. *J. Solid State Chem.* **1991**, 90, 216.
6. Kuhn, A.; Menendez, N.; Garcia-Alvarado, F.; Moran, E.; Tomero, J. D.; Alario-Franco, M. A. *J. Solid State Chem.* **1997**, 130, 184.
7. Kuhn, A.; Leon, C.; Garcia-Alvarado, F.; Santamaria, J.; Moran, E.; Alario-Franco, M. A. *J. Solid State Chem.* **1998**, 137, 168.
8. Shannon, R. D. *Acta Crystallogr.* **1976**, A32, 751.
9. Macdonald, J. R. *Impedance Spectroscopy*, John Wiley & Sons: New York, 1987.
10. Howell, F. S.; Bose, R. A.; Macedo, P. B.; Moynihan, C. T. *J. Phys. Chem.* **1974**, 78, 639.
11. Patel, H. K.; Martin, S. W. *Phys. Rev.* **1992**, B45, 10292.
12. Chowdari, B. V. R.; Gopalakrishnan, R. *Solid State Ionics* **1987**, 23, 225.
13. Bauerle, J. E. *J. Phys. Chem. Solids* **1969**, 30, 2657.
14. Macdonald, J. M. *LEI M ver 7.1.*, <http://www.physics.unc.edu/~macd>, 1999.
15. Pauling, L. *The Nature of the Chemical Bond*, 3rd ed.; Cornell Univ. Press: Ithaca, 1960.
16. Shin, Y. J.; Yi, M. Y. *Solid State Ionics* **2000** manuscript accepted.
17. Portier, J.; Campet, G.; Etourneau, J.; Tanguy, B. *J. Compounds and Alloys* **1994**, 209, 285.